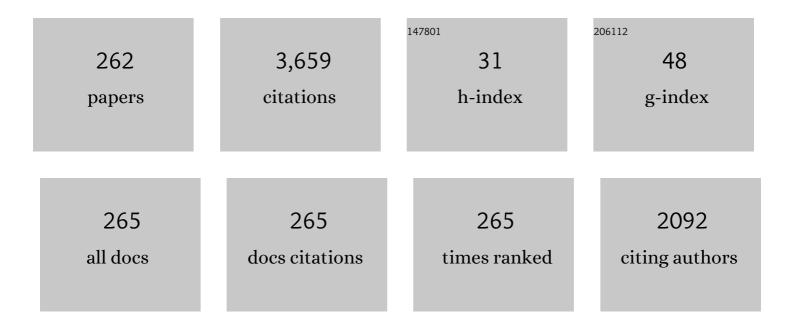
## Takaaki Manaka

List of Publications by Year in descending order

Source: https://exaly.com/author-pdf/4915702/publications.pdf Version: 2024-02-01



Τλέλλει Μλιλέλ

#	Article	IF	CITATIONS
1	Direct imaging of carrier motion in organic transistors by optical second-harmonic generation. Nature Photonics, 2007, 1, 581-584.	31.4	223
2	Analysis of pentacene field effect transistor as a Maxwell-Wagner effect element. Journal of Applied Physics, 2006, 100, 114515.	2.5	199
3	Probing of the electric field distribution in organic field effect transistor channel by microscopic second-harmonic generation. Applied Physics Letters, 2006, 89, 072113.	3.3	97
4	Maxwell–Wagner Model Analysis for the Capacitance–Voltage Characteristics of Pentacene Field Effect Transistor. Japanese Journal of Applied Physics, 2006, 45, 3712-3716.	1.5	81
5	Probing of carrier behavior in organic electroluminescent diode using electric field induced optical second-harmonic generation measurement. Applied Physics Letters, 2009, 95, .	3.3	66
6	Modulation in optical second harmonic generation signal from channel of pentacene field effect transistors during device operation. Applied Physics Letters, 2005, 87, 222107.	3.3	65
7	Diffusionlike electric-field migration in the channel of organic field-effect transistors. Physical Review B, 2008, 78, .	3.2	63
8	Electrophoretic Fabrication of Chitosanâ^'Zirconium-Oxide Nanobiocomposite Platform for Nucleic Acid Detection. Biomacromolecules, 2011, 12, 540-547.	5.4	62
9	Origin of electric field distribution in organic field-effect transistor: Experiment and analysis. Journal of Applied Physics, 2009, 105, .	2.5	59
10	Chiroptical switch based on azobenzene-substituted polydiacetylene LB films under thermal and photic stimuli. Journal of Materials Chemistry, 2010, 20, 285-291.	6.7	56
11	Analysis of Organic Light-Emitting Diode As a Maxwellâ^'Wagner Effect Element by Time-Resolved Optical Second Harmonic Generation Measurement. Journal of Physical Chemistry Letters, 2010, 1, 803-807.	4.6	55
12	Current-Voltage Characteristics of Pentacene Films: Effect of UV/Ozone Treatment on Au Electrodes. Japanese Journal of Applied Physics, 2005, 44, 561-565.	1.5	54
13	Control of the nano electrostatic phenomena at a pentacene/metal interface for improvement of the organic FET devices. Thin Solid Films, 2006, 499, 386-391.	1.8	51
14	Modeling of threshold voltage in pentacene organic field-effect transistors. Journal of Applied Physics, 2010, 107, .	2.5	48
15	The Charge Transport in Organic Field-Effect Transistor as an Interface Charge Propagation: The Maxwell–Wagner Effect Model and Transmission Line Approximation. Japanese Journal of Applied Physics, 2010, 49, 071603.	1.5	46
16	Analysis of Carrier Transients in Double-Layer Organic Light Emitting Diodes by Electric-Field-Induced Second-Harmonic Generation Measurement. Journal of Physical Chemistry C, 2010, 114, 15136-15140.	3.1	46
17	Analysis of Transient Currents in Organic Field Effect Transistor: The Time-of-Flight Method. Journal of Physical Chemistry C, 2009, 113, 18459-18461.	3.1	45
18	Orientational order study of monolayers at the air–water interface by Maxwell-displacement current and optical second harmonic generation. Journal of Chemical Physics, 2001, 115, 9010-9017.	3.0	44

#	Article	IF	CITATIONS
19	Analyzing carrier lifetime of double-layer organic solar cells by using optical electric-field-induced second-harmonic generation measurement. Applied Physics Letters, 2011, 98, .	3.3	44
20	Large surface potential of Alq3 film and its decay. Journal of Applied Physics, 2005, 97, 023703.	2.5	43
21	Preparation of Chiral Polydiacetylene Film from Achiral Monomers Using Circularly Polarized Light. Chemistry Letters, 2006, 35, 1028-1029.	1.3	39
22	Resonant enhancement of second-harmonic generation of electric quadrupole origin in phthalocyanine films. Physical Review B, 1996, 53, R13314-R13317.	3.2	37
23	Optical second-harmonic generation measurement for probing organic device operation. Light: Science and Applications, 2016, 5, e16040-e16040.	16.6	37
24	Studying Transient Carrier Behaviors in Pentacene Field Effect Transistors Using Visualized Electric Field Migration. Journal of Physical Chemistry C, 2009, 113, 10279-10284.	3.1	36
25	Probing of interfacial charging and discharging in double-layer devices with a polyimide blocking layer by time-resolved optical second harmonic generation. Journal of Applied Physics, 2010, 108, .	2.5	35
26	Investigation of interfacial charging and discharging in double-layer pentacene-based metal-insulator-metal device with polyterpenol blocking layer using electric field induced second harmonic generation. Chemical Physics Letters, 2011, 503, 105-111.	2.6	34
27	Electron-blocking hole-transport polyterpenol thin films. Chemical Physics Letters, 2012, 528, 26-28.	2.6	34
28	Analysis of carrier injection into a pentacene field effect transistor by optical second harmonic generation measurements. Journal of Applied Physics, 2007, 101, 024515.	2.5	33
29	Interaction of interfacial charge and ferroelectric polarization in a pentacene/poly(vinylidene) Tj ETQq1 1 0.7843	14 <sub>ქg</sub> BT /C	)veglock 10 Ti
30	Investigation of the Electrostatic Phenomena at Pentacene/Metal Interface by Second-Harmonic Generation. Japanese Journal of Applied Physics, 2005, 44, 2818-2822.	1.5	31
31	Influence of traps on transient electric field and mobility evaluation in organic field-effect transistors. Journal of Applied Physics, 2010, 107, 043712.	2.5	31
32	Probing of electric field in pentacene using microscopic optical second harmonic generation. Journal of Applied Physics, 2008, 103, 084118.	2.5	29
33	Insight into the contact resistance problem by direct probing of the potential drop in organic field-effect transistors. Applied Physics Letters, 2010, 97, .	3.3	29
34	Analysis of hysteresis behavior of pentacene field effect transistor characteristics with capacitance-voltage and optical second harmonic generation measurements. Journal of Applied Physics, 2007, 101, 094505.	2.5	28
35	Probing interfacial charge accumulation in ITO/α-NPD/Alq3/Al diodes under two electroluminescence operational modes by electric-field induced optical second-harmonic generation. Journal of Applied Physics, 2012, 112, .	2.5	28
36	Optical second harmonic generation imaging for visualizing in-plane electric field distribution. Optics Express, 2007, 15, 15964.	3.4	27

#	Article	IF	CITATIONS
37	Spectroscopic consideration of the surface potential built across phthalocyanine thin films on a metal electrode. Journal of Chemical Physics, 2004, 120, 7725-7732.	3.0	26
38	Probing and modeling of interfacial carrier motion in organic devices by optical second harmonic generation. Journal of Vacuum Science and Technology B:Nanotechnology and Microelectronics, 2010, 28, C5F12-C5F16.	1.2	26
39	Probing carrier injection into pentacene field effect transistor by time-resolved microscopic optical second harmonic generation measurement. Journal of Applied Physics, 2009, 106, 014511.	2.5	25
40	Fabricating chiral polydiacetylene film by monolayer compression and circularly polarized ultra-violet light. Chemical Physics Letters, 2007, 442, 97-100.	2.6	24
41	Thermionic emission model for contact resistance in organic field-effect transistor. Thin Solid Films, 2009, 518, 795-798.	1.8	24
42	Analyzing photovoltaic effect of double-layer organic solar cells as a Maxwell-Wagner effect system by optical electric-field-induced second-harmonic generation measurement. Journal of Applied Physics, 2011, 110, .	2.5	24
43	Analyzing photo-induced interfacial charging in IZO/pentacene/C60/bathocuproine/Al organic solar cells by electric-field-induced optical second-harmonic generation measurement. Journal of Applied Physics, 2012, 111, .	2.5	24
44	Study of blocking effect of Cu-phthalocyanine layer in zinc oxide/pentacene/CuPc/C60/Al organic solar cells by electric field-induced optical second harmonic generation measurement. Organic Electronics, 2013, 14, 320-325.	2.6	24
45	Channel Formation as an Interface Charging Process in a Pentacene Field Effect Transistor Investigated by Time-Resolved Second Harmonic Generation and Impedance Spectroscopy. Japanese Journal of Applied Physics, 2012, 51, 02BK08.	1.5	24
46	Instrument equipped with Maxwell displacement current and optical second-harmonic generation measurement system. Review of Scientific Instruments, 2003, 74, 2828-2835.	1.3	23
47	Determination of the complete dielectric polarization of Langmuir monolayers. Review of Scientific Instruments, 2005, 76, 083902.	1.3	23
48	Analysis of interface carrier accumulation and relaxation in pentacene/C60 double-layer organic solar cell by impedance spectroscopy and electric-field-induced optical second harmonic generation. Journal of Applied Physics, 2011, 110, .	2.5	23
49	Charge injection and accumulation in organic light-emitting diode with PEDOT:PSS anode. Journal of Applied Physics, 2015, 117, .	2.5	23
50	Decay process of a large surface potential of Alq3 films by heating. Journal of Applied Physics, 2006, 100, 053707.	2.5	22
51	Direct observation of trapped carriers in polydiacetylene films by optical second harmonic generation. Applied Physics Letters, 2007, 90, 171119.	3.3	22
52	Injected carrier distribution in a pentacene field effect transistor probed using optical second harmonic generation. Journal of Applied Physics, 2008, 104, .	2.5	22
53	Second-Harmonic Generation inC70Film. Japanese Journal of Applied Physics, 1997, 36, 6403-6404.	1.5	21
54	Analysis of pentacene field-effect transistor with contact resistance as an element of a Maxwell–Wagner effect system. Journal of Applied Physics, 2008, 104, .	2.5	21

#	Article	IF	CITATIONS
55	Detection of phase transition of monolayers at the air–water interface by compression using Maxwell displacement current and optical second harmonic generation. Journal of Chemical Physics, 2003, 118, 5640-5649.	3.0	20
56	Analyzing interfacial carrier charging in pentacene/C60 double-layer organic solar cells by optical electric field induced second-harmonic generation measurement. Chemical Physics Letters, 2011, 511, 491-495.	2.6	20
57	Second-harmonic generation and Maxwell displacement current spectroscopy of chiral organic monolayers at the air–water interface. Journal of Chemical Physics, 2003, 119, 7427-7434.	3.0	19
58	Carrier injection and transport in organic field-effect transistor investigated by impedance spectroscopy. Thin Solid Films, 2009, 518, 448-451.	1.8	19
59	Electrostatic energies stored in dipolar films and analysis of decaying process of a large surface potential of Alq3 films. Chemical Physics Letters, 2006, 430, 340-344.	2.6	18
60	Study of phase transition of two-dimensional ferroelectric copolymer P(VDF-TrFE) Langmuir monolayer by Maxwell displacement current and Brewster angle microscopy. Journal of Chemical Physics, 2009, 131, .	3.0	18
61	Bulk-trap modulated Maxwell-Wagner type interfacial carrier relaxation process in a fullerene/polyimide double-layer device investigated by time-resolved second harmonic generation. Journal of Applied Physics, 2011, 110, .	2.5	18
62	Selective observation of photo-induced electric fields inside different material components in bulk-heterojunction organic solar cell. Applied Physics Letters, 2014, 104, .	3.3	18
63	Stability in 3D and 2D/3D hybrid perovskite solar cells studied by EFISHG and IS techniques under light and heat soaking. Organic Electronics, 2019, 66, 7-12.	2.6	18
64	Highly Aligned α-Type Copper Phthalocyanine Formed on Rubbed Polyimide Alignment Layer. Japanese Journal of Applied Physics, 2000, 39, 4910-4911.	1.5	17
65	Probing of channel region in pentacene field effect transistors by optical second harmonic generation. Chemical Physics Letters, 2009, 477, 221-224.	2.6	17
66	Direct Observation of Anisotropic Carrier Transport in Organic Semiconductor by Time-Resolved Microscopic Optical Second-Harmonic Imaging. Applied Physics Express, 2013, 6, 101601.	2.4	17
67	Current collapse imaging of Schottky gate AlGaN/GaN high electron mobility transistors by electric field-induced optical second-harmonic generation measurement. Applied Physics Letters, 2014, 104, 252112.	3.3	17
68	Displacement current analysis of carrier behavior in pentacene field effect transistor with poly(vinylidene fluoride and tetrafluoroethylene) gate insulator. Journal of Applied Physics, 2009, 106, 024505.	2.5	16
69	Transport limited interfacial carrier relaxation in a double-layer device investigated by time-resolved second harmonic generation and impedance spectroscopy. Applied Physics Letters, 2011, 98, .	3.3	16
70	Direct probing of contact electrification by using optical second harmonic generation technique. Scientific Reports, 2015, 5, 13019.	3.3	16
71	Modeling and visualization of carrier motion in organic films by optical second harmonic generation and Maxwell-displacement current. Journal Physics D: Applied Physics, 2015, 48, 373001.	2.8	16
72	Effect of nanoparticles concentration on electromagnetic-assisted oil recovery using ZnO nanofluids. PLoS ONE, 2020, 15, e0244738.	2.5	16

#	Article	IF	CITATIONS
73	Surface Morphology and Electrical Transport Properties of Polydiacetylene-Based Organic Field-Effect Transistors. Japanese Journal of Applied Physics, 2006, 45, 6436-6441.	1.5	15
74	Investigation of space charge at pentacene/metal interfaces by a near-field scanning microwave microprobe. Applied Physics Letters, 2007, 90, 182104.	3.3	15
75	Probing Electric Field Distribution in Underlayer of an Organic Double-Layer System by Optical Second-Harmonic Generation Measurement. Japanese Journal of Applied Physics, 2009, 48, 021504.	1.5	15
76	Space charge field effect on light emitting from tetracene field-effect transistor under AC electric field. Thin Solid Films, 2009, 518, 583-587.	1.8	15
77	Observation of electron behavior in ambipolar polymer-based light-emitting transistor by optical second harmonic generation. Journal of Applied Physics, 2011, 110, 013715.	2.5	15
78	Algal Biophotovoltaic Devices: Surface Potential Studies. ACS Sustainable Chemistry and Engineering, 2020, 8, 10511-10520.	6.7	15
79	Domain observation and molecular orientation of chiral dipalmitoylphosphatidylcholine monolayer by Brewster angle microscopy and Maxwell displacement current. Thin Solid Films, 2008, 516, 2649-2651.	1.8	14
80	Study of trap-filling effect on transient carrier transport in pentacene field effect transistors by time-resolved optical second harmonic generation. Chemical Physics Letters, 2011, 507, 195-198.	2.6	14
81	Direct probing of the selective electron and hole accumulation at organic/organic interfaces in a triple-layer organic device by time-resolved optical second harmonic generation. Applied Physics Letters, 2011, 99, 083301.	3.3	14
82	Probing and modeling of carrier motion in organic devices by electric-field-induced optical second-harmonic generation. Japanese Journal of Applied Physics, 2014, 53, 100101.	1.5	14
83	Study of carrier transport in flexible organic field-effect transistors: Analysis of bending effect and microscopic observation using electric-field-induced optical second-harmonic generation. Thin Solid Films, 2014, 554, 166-169.	1.8	14
84	p- and n-Channel Photothermoelectric Conversion Based on Ultralong Near-Infrared Wavelengths Absorbing Polymers. ACS Applied Polymer Materials, 2019, 1, 542-551.	4.4	14
85	Contact Resistance as an Origin of the Channel-Length-Dependent Threshold Voltage in Organic Field-Effect Transistors. Japanese Journal of Applied Physics, 2012, 51, 100205.	1.5	14
86	Observation of the lowest Ag excited state lying in the optical gap in polydiacetylene by means of second-harmonic generation spectroscopy. Synthetic Metals, 1998, 95, 155-158.	3.9	13
87	Orientational order study of 4-alkyl-4′-cyanobiphenyl Langmuir films by Maxwell displacement current and optical second harmonic generation measurements. Thin Solid Films, 2001, 393, 86-91.	1.8	13
88	Investigation of the surface potential formed in Alq3 films on metal surface by Kelvin probe and nonlinear optical measurement. Current Applied Physics, 2006, 6, 877-881.	2.4	13
89	Evaluation of carrier velocity using time-resolved optical second harmonic generation measurement. Applied Physics Letters, 2008, 92, .	3.3	13
90	Molecular structure modulated properties of azobenzene-substituted polydiacetylene LB films: Chirality formation and thermal stability. Polymer, 2010, 51, 2229-2235.	3.8	13

#	Article	IF	CITATIONS
91	Reduction of Hysteresis in Organic Field-Effect Transistor by Ferroelectric Gate Dielectric. Japanese Journal of Applied Physics, 2010, 49, 021601.	1.5	13
92	Analysis of carrier injection, accumulation and transport process of pentacene field effect transistors using a Maxwell–Wagner model. Current Applied Physics, 2007, 7, 356-359.	2.4	12
93	Analysis of threshold voltage shift of pentacene field effect transistor with ferroelectric gate insulator as a Maxwell–Wagner effect. Thin Solid Films, 2008, 516, 2753-2757.	1.8	12
94	Probing motion of electric dipoles and carriers in organic monolayers by Maxwell Displacement Current and optical second harmonic generation. Thin Solid Films, 2008, 517, 1312-1316.	1.8	12
95	Observation of Carrier Behavior in Organic Field-Effect Transistors with Electroluminescence under AC Electric Field. Japanese Journal of Applied Physics, 2008, 47, 3200-3203.	1.5	12
96	Effect of external electrostatic charge on condensed phase domains at the air-water interface: Experiment and shape equation analysis. Journal of Chemical Physics, 2009, 130, 104706.	3.0	12
97	Trapping effect of metal nanoparticle mono- and multilayer in the organic field-effect transistor. Journal of Applied Physics, 2011, 109, 064512.	2.5	12
98	Analyzing two electroluminescence modes of indium tin oxide/α-NPD/Alq3/Al diodes by using large alternating current square voltages. Journal of Applied Physics, 2011, 110, 103707.	2.5	12
99	Analyzing hysteresis behavior of capacitance–voltage characteristics of IZO/C60/pentacene/Au diodes with a hole-transport electron-blocking polyterpenol layer by electric-field-induced optical second-harmonic generation measurement. Chemical Physics Letters, 2013, 572, 150-153.	2.6	12
100	Determination of dipole moment of azobenzene dendrimer by Maxwell-displacement-current measurement for Langmuir monolayer. Chemical Physics Letters, 2002, 355, 164-168.	2.6	11
101	Electrical Transport Properties of Polydiacetylene Films during Thermochromic Process. Japanese Journal of Applied Physics, 2007, 46, 3071-3076.	1.5	11
102	Electrostatic Maxwell stress model of the shapes of condensed phase domains in monolayers at the air-water interface. Journal of Chemical Physics, 2008, 128, 204706.	3.0	11
103	Study of Carrier Behavior in Pentacene in a Au/Pentacene/Ferroelectric Poly(vinylidene) Tj ETQq1 1 0.784314 rgBT Generation Measurement. Japanese Journal of Applied Physics, 2010, 49, 121601.	/Overlock 1.5	10 Tf 50 2( 11
104	Study of relaxation process of dipalmitoyl phosphatidylcholine monolayers at air–water interface: Effect of electrostatic energy. Journal of Chemical Physics, 2011, 134, 154709.	3.0	11
105	The Maxwell-Wagner model for charge transport in ambipolar organic field-effect transistors: The role of zero-potential position. Applied Physics Letters, 2012, 101, 243302.	3.3	11
106	Observation of Electron Injection into Organic Field-Effect Transistor with Au Electrodes using Electroluminescence under AC Electric Field. Japanese Journal of Applied Physics, 2008, 47, 1297-1300.	1.5	10
107	Trapping centers engineering by including of nanoparticles into organic semiconductors. Journal of Applied Physics, 2008, 104, 114502.	2.5	10
108	Induced Optical Chirality of Poly(diacetylene) Film by Circularly Polarized Light and Its Control by Changing Substrate Temperature. Japanese Journal of Applied Physics, 2008, 47, 1359-1362.	1.5	10

#	Article	IF	CITATIONS
109	Effect of an Upward and Downward Interface Dipole Langmuir–Blodgett Monolayer on Pentacene Organic Field-Effect Transistors: A Comparison Study. Japanese Journal of Applied Physics, 2012, 51, 024102.	1.5	10
110	Analyzing a two-step polarization process in a pentacene/poly(vinylidene fluoride - trifluoroethylene) double-layer device using Maxwell-Wagner model. Journal of Applied Physics, 2012, 111, 023706.	2.5	10
111	Direct observation of trapped charges under field-plate in p-GaN gate AlGaN/GaN high electron mobility transistors by electric field-induced optical second-harmonic generation. Applied Physics Letters, 2017, 110, .	3.3	10
112	Detection of flexoelectric effect from 4-heptyloxy-4′-cyanobiphenyl monolayers at an air-water interface by Maxwell displacement current and optical second harmonic generation. Journal of Chemical Physics, 2005, 122, 164703.	3.0	9
113	Pentacene field effect transistor as an injection-type element: Maxwell–Wagner type interfacial polarization and carrier transport. Current Applied Physics, 2007, 7, 334-337.	2.4	9
114	Mobility Measurement Based on Visualized Electric Field Migration in Organic Field-Effect Transistors. Applied Physics Express, 0, 2, 061501.	2.4	9
115	Carrier injection from polypyrrole coated gold electrode in pentacene field effect transistors. Synthetic Metals, 2010, 160, 2116-2120.	3.9	9
116	Three-dimensional current collapse imaging of AlGaN/GaN high electron mobility transistors by electric field-induced optical second-harmonic generation. Applied Physics Letters, 2016, 109, .	3.3	9
117	Observation of the Electric-Dipole-Forbidden States in Polydiacetylene by Means of Resonance Second-Harmonic Generation Spectroscopy. Japanese Journal of Applied Physics, 1996, 35, L832-L834.	1.5	8
118	Photoisomerization of Azobenzene Dendrimer Monolayer Investigated by Maxwell Displacement Current Technique. Japanese Journal of Applied Physics, 2001, 40, 7085-7090.	1.5	8
119	Second harmonic generation from copper-tetratert-butyl-phthalocyanine Langmuir–Blodgett film/metal interface: Electric quadrupole or electric field induced second harmonic generation effect?. Journal of Applied Physics, 2002, 92, 6390-6398.	2.5	8
120	Function of Interfacial Dipole Monolayer in Organic Field Effect Transistors. Japanese Journal of Applied Physics, 2011, 50, 04DK10.	1.5	8
121	Direct probing of selective electron and hole accumulation processes along the channel of an ambipolar double-layer field-effect transistor by optical modulation spectroscopy. Applied Physics Letters, 2012, 100, 103301.	3.3	8
122	Memory effect in organic transistor: Controllable shifts in threshold voltage. Chemical Physics Letters, 2012, 551, 105-110.	2.6	8
123	Thiol Modified Chitosan Self-Assembled Monolayer Platform for Nucleic Acid Biosensor. Applied Biochemistry and Biotechnology, 2014, 174, 1201-1213.	2.9	8
124	Electrostatic Properties of Polyethylene Langmuir-Blodgett films. Japanese Journal of Applied Physics, 2003, 42, 6473-6476.	1.5	7
125	In situObservations of Orientational Ordering Process of 4'-n-pentyl-4-cyanobiphenyl Ultra-Thin Film Using Polarized Absorption Measurements. Japanese Journal of Applied Physics, 2005, 44, 1037-1040.	1.5	7
126	Analysis of Threshold Voltage Shift of Pentacene Field Effect Transistor Based on a Maxwell–Wagner Effect. Japanese Journal of Applied Physics, 2007, 46, 2709-2713.	1.5	7

#	Article	IF	CITATIONS
127	Analysis of Pentacene Field-Effect Transistor with a Ferroelectric P(VDF–TeFE) Gate Insulator as an Element of Maxwell–Wagner Effect System. Japanese Journal of Applied Physics, 2009, 48, 021501.	1.5	7
128	Investigation of the Voltage Establishment and Relaxation Processes in a Double-Layer Device by Time-Resolved Optical Second-Harmonic Generation. Japanese Journal of Applied Physics, 2011, 50, 04DK13.	1.5	7
129	A Novel Microscope for Visualizing Electric Fields in Organic Thin Film Devices Using Electric-Field-Induced Second-Harmonic Generation. Japanese Journal of Applied Physics, 2013, 52, 04CK04.	1.5	7
130	Analysis of carrier behavior in C60/P(VDF-TrFE) double-layer capacitor by using electric-field-induced optical second-harmonic generation measurement. Journal of Applied Physics, 2013, 114, 234504.	2.5	7
131	Organic double layer element driven by triboelectric nanogenerator: Study of carrier behavior by non-contact optical method. Chemical Physics Letters, 2016, 646, 64-68.	2.6	7
132	Study of carrier energetics in ITO/P(VDF-TrFE)/pentacene/Au diode by using electric-field-induced optical second harmonic generation measurement and charge modulation spectroscopy. Journal of Applied Physics, 2017, 121, 065501.	2.5	7
133	Detection of the reversible flow behavior of 4-heptyloxy-4′-cyanobiphenyl monolayer at air–water interface by compression and expansion with Maxwell displacement current and optical second harmonic generation. Chemical Physics Letters, 2003, 378, 428-433.	2.6	6
134	Preparation and surface morphology change observation of hybrid bilayer membranes. Thin Solid Films, 2006, 499, 40-43.	1.8	6
135	The interacting electrostatic charge model on the shape formation of monolayer domains at the air–water interface comprised of tilted dipoles with orientational deformation. Thin Solid Films, 2008, 516, 2660-2665.	1.8	6
136	Investigation of space charge at pentacene/Au interface with UV/ozone treatment by a near-field microwave microprobe. Thin Solid Films, 2008, 516, 2573-2576.	1.8	6
137	Analysis of Charge Accumulation in Pentacene Feld Effect Transistor with Ferroelectric Gate Insulator using Maxwell–Wagner Model. Japanese Journal of Applied Physics, 2008, 47, 3170-3173.	1.5	6
138	Dipolar electrostatic energy effect on relaxation process of monolayers at air-water interface: Analysis of thermodynamics and kinetics. Journal of Chemical Physics, 2009, 131, 244709.	3.0	6
139	Probing the electric field in organic double layer-system by optical second harmonic generation. Thin Solid Films, 2009, 518, 893-895.	1.8	6
140	Effect of Photogenerated Carriers on Ferroelectric Polarization Reversal. Applied Physics Express, 2011, 4, 121601.	2.4	6
141	Probing electric field in double-layer electroluminescence diode by optical second harmonic generation. Chemical Physics Letters, 2011, 516, 254-256.	2.6	6
142	Vertical orientation with a narrow distribution of helical peptides immobilized on a quartz substrate by stereocomplex formation. Soft Matter, 2012, 8, 3387.	2.7	6
143	Study of interface layer effect in organic solar cells by electric-field-induced optical second-harmonic generation measurement. Thin Solid Films, 2014, 554, 51-53.	1.8	6
144	Modeling and analysis of I-V hysteresis behaviors caused by defects in tin perovskite thin films. Journal of Applied Physics, 2018, 124, .	2.5	6

#	Article	IF	CITATIONS
145	Role of Phase-Dependent Dielectric Properties of Alumina Nanoparticles in Electromagnetic-Assisted Enhanced Oil Recovery. Nanomaterials, 2020, 10, 1975.	4.1	6
146	Enhancement of Surface Potential Buildup and Decay of Tris(8-quinolinato)aluminum Film Deposited on Ultraviolet/Ozone-Treated Gold Electrodes. Japanese Journal of Applied Physics, 2005, 44, 1091-1094.	1.5	5
147	Orientational order of 4′-n-pentyl-4-cyanobiphenyl molecules deposited on azobenzene monolayers. Thin Solid Films, 2006, 499, 229-233.	1.8	5
148	Cooperative Molecular Field Effect on the Surface Potential of Tris(8-quinolinato)aluminum Films. Japanese Journal of Applied Physics, 2007, 46, 2740-2744.	1.5	5
149	Pentacene Field-Effect Transistor with Ferroelectric Gate Insulator as Maxwell–Wagner Effect Element. Japanese Journal of Applied Physics, 2008, 47, 476-479.	1.5	5
150	Study of Domain Shapes and Orientational Structure of Phospholipid Monolayers using Maxwell Displacement Current and Brewster Angle Microscopy. Japanese Journal of Applied Physics, 2008, 47, 411-415.	1.5	5
151	Optical Chirality Induced in Evaporated Poly(diacetylene) Film by Circularly Polarized Light. Macromolecular Symposia, 2008, 268, 77-80.	0.7	5
152	Modeling carrier transport and electric field evolution in Gaussian disordered organic field-effect transistors. Journal of Applied Physics, 2011, 109, 104512.	2.5	5
153	Channel Formation as an Interface Charging Process in a Pentacene Field Effect Transistor Investigated by Time-Resolved Second Harmonic Generation and Impedance Spectroscopy. Japanese Journal of Applied Physics, 2012, 51, 02BK08.	1.5	5
154	Study of carrier blocking property of poly-linalyl acetate thin layer by electric-field-induced optical second-harmonic generation measurement. Chemical Physics Letters, 2014, 593, 69-71.	2.6	5
155	Study of effect of inserted pentacene layer in ITO/P(VDF-TrFE)/α-NPD/Au capacitor using electric-field-induced optical second-harmonic generation and displacement current. Organic Electronics, 2014, 15, 537-542.	2.6	5
156	Analysis of current-voltage characteristics of Au/pentacene/fluorine polymer/indium zinc oxide diodes by electric-field-induced optical second-harmonic generation. Journal of Applied Physics, 2015, 117, .	2.5	5
157	Imaging of triboelectric charge distribution induced in polyimide film by using optical second-harmonic generation: Electronic charge distribution and dipole alignment. Applied Physics Letters, 2019, 114, 233301.	3.3	5
158	Electrostatic charge effect on the orientational distribution of molecules on the water surface. Chemical Physics Letters, 2003, 368, 370-376.	2.6	4
159	Study of Second Harmonic Generation from Copper-tetra-tert-butyl-phthalocyanine Langmüir-Blodgett Film/Metal Interface. Japanese Journal of Applied Physics, 2003, 42, 2516-2522.	1.5	4
160	Electrostatic properties of polyethylene LB films on metal electrodes. Colloids and Surfaces A: Physicochemical and Engineering Aspects, 2005, 257-258, 287-290.	4.7	4
161	Measurement of interfacial dielectric polarization for the investigation of the orientational structure of monolayers comprised of banana-shaped molecules at an air–water interface. Thin Solid Films, 2006, 499, 242-248.	1.8	4
162	Probing and modeling of carrier motion in organic devices by optical second harmonic generation. Thin Solid Films, 2010, 519, 961-963.	1.8	4

#	Article	IF	CITATIONS
163	Electroluminescence Generated from ITO/α-NPD/Alq <sub>3</sub> /Al Diodes by Applying A.C. Square Voltage. Molecular Crystals and Liquid Crystals, 2012, 567, 187-192.	0.9	4
164	Probing a two-step channel formation process in injection-type pentacene field-effect transistors by time-resolved electric-field-induced optical second-harmonic generation measurement. Organic Electronics, 2012, 13, 2801-2806.	2.6	4
165	Multiple-trapping in pentacene field-effect transistors with a nanoparticles self-assembled monolayer. AIP Advances, 2012, 2, .	1.3	4
166	Interfacial charging of copper phthalocyanine/C60 double-layer organic solar cells induced by photoillumination: Effect of photoconductivity change. Thin Solid Films, 2014, 554, 158-161.	1.8	4
167	Determination of carrier mobility of semiconductor layer in organic metal-insulator-semiconductor diodes by displacement current and electric-field-induced optical second-harmonic generation measurements. Organic Electronics, 2017, 43, 70-76.	2.6	4
168	Degradation analysis of AlGaN/GaN high electron mobility transistor by electroluminescence, electric field-induced optical second-harmonic generation, and photoluminescence imaging. Applied Physics Letters, 2018, 113, .	3.3	4
169	Dipolar polarization as an energy source of tribo-electric power generator. Applied Physics Letters, 2021, 119, .	3.3	4
170	Effect of an Upward and Downward Interface Dipole Langmuir–Blodgett Monolayer on Pentacene Organic Field-Effect Transistors: A Comparison Study. Japanese Journal of Applied Physics, 2012, 51, 024102.	1.5	4
171	Interfacial polarization phenomena in organic molecular films. Analytica Chimica Acta, 2006, 568, 65-69.	5.4	3
172	Investigation of Pentacene Field-Effect Transistor Operation by Optical Second-Harmonic Generation. Japanese Journal of Applied Physics, 2007, 46, 2687-2691.	1.5	3
173	Preparation of chiral poly(diacetylene) films from 10,12-pentacosadiynoic acid using circularly polarized light. Thin Solid Films, 2009, 518, 842-844.	1.8	3
174	Electrochemical methods coupled with impedance measurement for energy gap study: correlation between the energy states and charge transport properties. Synthetic Metals, 2012, 162, 2236-2241.	3.9	3
175	Investigation of carrier transit motion in PCDTBT by optical SHG technique. Laser Physics, 2014, 24, 105701.	1.2	3
176	Probing space charge effect on electroluminescence of indium tin oxide (ITO)/N,Nâ€2-di-[(1-naphthyl)-N,Nâ€2-diphenyl]-(1,1â€2-biphenyl)-4, 4â€2-diamine (α-NPD)/tris(8-hydroxy-quinolin aluminum (III) (Alq3)/Al diodes by time-resolved electric-field-induced optical second-harmonic generation measurement. Thin Solid Films, 2014, 554, 110-113.	iato) 1.8	3
177	Probing of Electric Field Distribution and Carrier Behavior in Double-Layer Organic Light-Emitting Diodes by a Novel Microscopic Electric-Field-Induced Optical Second-Harmonic Generation Measurement system. Transactions of the Materials Research Society of Japan, 2014, 39, 443-446.	0.2	3
178	Evaluation of Thermal Stability of Organic Electro-Optic Device by Using Thermally Stimulated Current. Journal of Nanoscience and Nanotechnology, 2016, 16, 3378-3382.	0.9	3
179	Optical second harmonic generation spectra in vacuumâ€deposited thin films of various phthalocyanines. Journal of Porphyrins and Phthalocyanines, 1998, 2, 133-137.	0.8	3
180	Investigation of the Voltage Establishment and Relaxation Processes in a Double-Layer Device by Time-Resolved Optical Second-Harmonic Generation. Japanese Journal of Applied Physics, 2011, 50, 04DK13.	1.5	3

#	Article	IF	CITATIONS
181	Photoinduced Gate Modulation and Temperature Dependence in the Coulomb Staircase of Organic Single Electron Tunneling Junctions. Japanese Journal of Applied Physics, 2004, 43, 2357-2361.	1.5	2
182	Optical chirality of citronelloxy-cyanobiphenyl monolayer at an air–water interface studied by the MDC and SHG measurement. Chemical Physics Letters, 2005, 407, 337-341.	2.6	2
183	Study of interfacial polarization phenomena in organic films by MDC, SHG and surface potential measurement. Current Applied Physics, 2005, 5, 317-320.	2.4	2
184	Analysis of polar orientational order controlled by nanometer-thick polyimide Langmuir-Blodgett films. Chemical Physics Letters, 2007, 449, 138-143.	2.6	2
185	Study of electrostatic energy contribution on monolayer domains size. Thin Solid Films, 2008, 517, 1317-1320.	1.8	2
186	Optical second harmonic generation measurements for investigating electron injection into a pentacene field effect transistor with Au source and drain electrodes. Thin Solid Films, 2008, 516, 2513-2517.	1.8	2
187	Probing of Channel Formation in Organic Field-Effect Transistors by Optical Second Harmonic Generation Measurement. Japanese Journal of Applied Physics, 2008, 47, 3179-3184.	1.5	2
188	Orientational Reordering of Liquid Crystalline Monolayers by Cooperative Molecular Field Effect. Japanese Journal of Applied Physics, 2008, 47, 3142-3146.	1.5	2
189	Charge Storage and Carrier Transport at Organic Semiconductor-Insulator Interface. Hyomen Kagaku, 2008, 29, 105-113.	0.0	2
190	Transient charge accumulation in pentacene field effect transistor with silver electrode. Thin Solid Films, 2009, 518, 485-488.	1.8	2
191	Solid polymerization and supramolecular chirality formation of azobenzene substituted diacetylene Langmuir–Blodgett films. Thin Solid Films, 2009, 518, 750-753.	1.8	2
192	Effect of orientational order of tris(8-hydroxyquinolinato)aluminum(III) on electroabsorption. Thin Solid Films, 2009, 518, 754-757.	1.8	2
193	Effect of Traps on Carrier Injection and Transport in Organic Fieldâ€effect Transistor. IEEJ Transactions on Electrical and Electronic Engineering, 2010, 5, 391-394.	1.4	2
194	Electroluminescence Enhanced from Electrode Interface in ITO/Tetracene/Al Diodes. Molecular Crystals and Liquid Crystals, 2011, 538, 112-117.	0.9	2
195	Conservation of the injection and transit time ratio in organic field-effect transistors: A thermally accelerated aging study. Journal of Applied Physics, 2012, 111, 104505.	2.5	2
196	Direct Probing of Internal Electric-fields in Fullerene Diodes Using Electric-field-induced Second-harmonic Generation Measurement. Molecular Crystals and Liquid Crystals, 2013, 578, 50-54.	0.9	2
197	Master equation model for Gaussian disordered organic field-effect transistors. Journal of Applied Physics, 2013, 114, 074502.	2.5	2
198	Impact of the interfacial traps on the charge accumulation in organic transistors. Journal of Experimental Nanoscience, 2014, 9, 994-1002.	2.4	2

#	Article	IF	CITATIONS
199	Visualizing polarization structure of lipid Langmuir monolayer by surface second-harmonic generation technique. Thin Solid Films, 2014, 554, 8-12.	1.8	2
200	Interfacial charging originated from the conductivity decrease of C60 layer in IZO/pentacene/C60/Al organic double-layer solar cells. Organic Electronics, 2014, 15, 162-168.	2.6	2
201	Metal nanoparticles in organic field-effect transistor: Transition from charge trapping to conduction mechanism. Thin Solid Films, 2014, 554, 189-193.	1.8	2
202	Direct visualization and modeling of carrier distribution in organic light emitting transistor. Thin Solid Films, 2014, 554, 162-165.	1.8	2
203	Observation of turnover of spontaneous polarization in ferroelectric layer of pentacene/poly-(vinylidene-trifluoroethylene) double-layer capacitor under photo illumination by optical second-harmonic generation measurement. Journal of Applied Physics, 2016, 119, 165502.	2.5	2
204	Direct visualization of polarization reversal of organic ferroelectric memory transistor by using charge modulated reflectance imaging. Journal of Applied Physics, 2017, 122, 185501.	2.5	2
205	Study of I-V Hysteresis of Tin Perovskite Solar Cells Using Capacitance-Voltage Measurement Coupled with Charge Modulation Spectroscopy. Molecular Crystals and Liquid Crystals, 2019, 686, 92-98.	0.9	2
206	Visualizing Positive and Negative Charges of Triboelectricity Generated on Polyimide Film. IEICE Transactions on Electronics, 2021, E104.C, 170-175.	0.6	2
207	A Novel Electric Field Induced Optical Second Harmonic Generation Technique for Visualizing Carrier-dynamics in Organic Electronics Materials. IEEJ Transactions on Fundamentals and Materials, 2016, 136, 678-684.	0.2	2
208	Function of Interfacial Dipole Monolayer in Organic Field Effect Transistors. Japanese Journal of Applied Physics, 2011, 50, 04DK10.	1.5	2
209	Study of Orientational Order Parameters of 4-Octyl-4'-N-cyanobiphenyl langmuir films by Maxwell displacement current measurement coupled with Optical Second Harmonic Generation Measurement. Molecular Crystals and Liquid Crystals, 2004, 412, 189-196.	0.9	1
210	Analysis of Organic Field Effect Transistors as a Maxwell-Wagner Effect Element: Measurement of Nano-Interfacial Polarization and Electric Field Distribution in Organic Film by Optical Second Harmonic Generation. Molecular Crystals and Liquid Crystals, 2007, 467, 285-293.	0.9	1
211	Optical Second-Harmonic Generation Measurements of Hole Carrier Injection and Trapping in Pentacene Field-Effect Transistor. Japanese Journal of Applied Physics, 2007, 46, 2722-2726.	1.5	1
212	Observation of orientational ordering processes of 4-n-pentyl-4′-cyanobiphenyl molecules during evaporation onto polyimide Langmuir–Blodgett films by optical polarized absorption measurements. Thin Solid Films, 2008, 516, 2656-2659.	1.8	1
213	Observation of channel formation carriers in pentacene field-effect transistor by electric field induced optical second harmonic generation. Thin Solid Films, 2008, 517, 1321-1323.	1.8	1
214	Orientational ordering of 4-pentyl-4′-cyanobiphenyl molecules evaporated on multi-layered polyimide film. Thin Solid Films, 2008, 517, 1407-1410.	1.8	1
215	Trapping centers engineering by including of nanoparticles into organic semiconductors. , 2008, , .		1
216	Transient Optical Second-Harmonic Generation Measurement for Monitoring Carrier Injection into Organic Field-Effect Transistors. Japanese Journal of Applied Physics, 2008, 47, 1301-1306.	1.5	1

#	Article	IF	CITATIONS
217	Preparation and Characterization of Micro-patterned Hybrid Bilayer Membrane. Transactions of the Materials Research Society of Japan, 2008, 33, 99-102.	0.2	1
218	Preparation and atomic force microscopy observation of lipid membranes on micro-patterned self-assembled monolayers. Thin Solid Films, 2009, 517, 3227-3229.	1.8	1
219	Effect of Trap Density on Carrier Propagation in Organic Field-Effect Transistors Investigated by Impedance Spectroscopy. Japanese Journal of Applied Physics, 2010, 49, 01AE14.	1.5	1
220	Probing of Electric Field Distribution in ITO/PI/P3HT/Au Using Electric Field Induced Second Harmonic Generation. IEICE Transactions on Electronics, 2011, E94-C, 185-186.	0.6	1
221	Maxwell-Wagner type interfacial relaxation process in a doublelayer device investigated by time and frequency domain approaches. Physics Procedia, 2011, 14, 46-51.	1.2	1
222	Analyzing Open-Voltage of Double-Layer Organic Solar Cells Using Optical Electric-Field-Induced Second-Harmonic Generation. Materials Research Society Symposia Proceedings, 2012, 1390, 118.	0.1	1
223	Analysis of Carrier Behaviors in Organic Field Effect Transistors. Hyomen Kagaku, 2012, 33, 75-80.	0.0	1
224	Mechanical strains modulate the carrier behaviors of organic field effect transistors. Journal of Applied Physics, 2012, 111, 054502.	2.5	1
225	Influence of Pentacene Interface Layer in ITO/-NPD/Alq3/Al Organic Light Emitting Diodes by Time-Resolved Electric-Field-Induced Optical Second-Harmonic Generation Measurement. Journal of Nanoscience and Nanotechnology, 2016, 16, 3188-3193.	0.9	1
226	Preparation of Chiral Polydiacetylene Films by Using Three-Photon Polymerization. Journal of Nanoscience and Nanotechnology, 2016, 16, 3394-3397.	0.9	1
227	Study of carrier-mobility of organic thin film by dark-injection time-of-flight and electric-field-induced optical second-harmonic generation measurements. Chemical Physics Letters, 2017, 677, 50-54.	2.6	1
228	Direct evaluation of anisotropic carrier mobility in uniaxially aligned polymer semiconductor film by time-resolved microscopic optical second-harmonic generation measurement. Journal Physics D: Applied Physics, 2017, 50, 015103.	2.8	1
229	Transient carrier visualization of organic-inorganic hybrid perovskite thin films by using time-resolved microscopic second-harmonic generation (TRM-SHC). Organic Electronics, 2019, 75, 105416.	2.6	1
230	Direct observation of carrier transport in organic–inorganic hybrid perovskite thin film by transient photoluminescence imaging measurement. Japanese Journal of Applied Physics, 2019, 58, SBBG18.	1.5	1
231	Effect of 1,8-Diiodooctance additive on the charge carriers behavior in the PCPDTBT:PC71BM BHJ films investigated by using electric-field-induced optical second-harmonic generation measurement. Journal of Materials Science: Materials in Electronics, 2021, 32, 2845-2852.	2.2	1
232	Probing of Carrier Injection into Organic Field Effect Transistor by Optical Second Harmonic Generation. IEEJ Transactions on Fundamentals and Materials, 2007, 127, 261-264.	0.2	1
233	Spectroscopic Study of Electric Field Induced Optical Second Harmonic Generation from PCPDTBT and PC <sub>71</sub> BM Thin Films. IEICE Transactions on Electronics, 2019, E102.C, 119-124.	0.6	1
234	Orientational Ordering Process of Liquid Crystalline Molecules Evaporated on Azobenzene Monolayer: Optical Polarized Absorption Measurements and Adsorption Kinetics. International Journal of the Society of Materials Engineering for Resources, 2006, 13, 109-111.	0.1	1

#	Article	IF	CITATIONS
235	Interfacial electrostatic phenomena in polyimide Langmuir–Blodgett films in electron tunneling devices. Current Applied Physics, 2003, 3, 223-226.	2.4	0
236	SHG-MDC SPECTROSCOPY FOR LIQUID CRYSTAL MONOLAYERS. Molecular Crystals and Liquid Crystals, 2003, 400, 1-11.	0.9	0
237	PHOTOINDUCED MOLECULAR MOTION OF THE AZOBENZENE MONOLAYER INVESTIGATED BY MAXWELL DISPLACEMENT CURRENT TECHNIQUE. Molecular Crystals and Liquid Crystals, 2004, 413, 63-69.	0.9	0
238	Surface Polarization in Interfacial Monolayer and SHG-MDC Spectroscopy. Molecular Crystals and Liquid Crystals, 2004, 424, 7-15.	0.9	0
239	Detection of Phase Transition of 4-Heptyloxy-4'-n-Cyanobiphenyl Langmuir Films By Maxwell Displacement Current and Optical Second Harmonic Generation Measurement. Molecular Crystals and Liquid Crystals, 2004, 412, 197-203.	0.9	0
240	Detection of nano-interfacial space charge field at metal–organic film interface by SHG and surface potential. Current Applied Physics, 2005, 5, 171-173.	2.4	0
241	Nanometric Interfacial Polarization Phenomena in Organic Monolayer Films Studied by Maxwell Displacement Current-Second Harmonic Generation Spectroscopy. Japanese Journal of Applied Physics, 2005, 44, 519-522.	1.5	Ο
242	Generation of Maxwell displacement current across 10, 12- tricosadynoic acid monolayer before and after polymerization. Thin Solid Films, 2006, 509, 94-101.	1.8	0
243	Manipulation of two dimensional interface. Thin Solid Films, 2006, 509, 69-74.	1.8	Ο
244	Contribution of Electrostatic Energy to Curvature and Frank Elastic Energy of Monolayer Domains Comprised of Polar Molecules: Shape of Domains with Orientational Deformation. Molecular Crystals and Liquid Crystals, 2007, 479, 33/[1071]-47/[1085].	0.9	0
245	Compression Induced Achiral-Chiral Phase Transition of Monolayers Comprised of Banana-Shaped Achiral Molecules at the Air-Water Interface: Importance of In-plane Nematic Order. Molecular Crystals and Liquid Crystals, 2007, 479, 13/[1051]-31/[1069].	0.9	Ο
246	Hole trapping in polydiacetylene field effect transistor studied by optical second harmonic generation. Thin Solid Films, 2008, 516, 2779-2782.	1.8	0
247	Spontaneous Orientational Ordering of Liquid Crystal Layer During Evaporation onto Silica. Molecular Crystals and Liquid Crystals, 2009, 512, 100/[1946]-108/[1954].	0.9	Ο
248	Direct Observation of Electron Transit in Ambipolar Polymer-Based Light-Emitting Transistor by Optical Second Harmonic Generation Measurement. Physics Procedia, 2011, 14, 226-230.	1.2	0
249	Study of Electrical Conduction Mechanism of Organic Double-Layer Diode Using Electric Field Induced Optical Second Harmonic Generation Measurement. Journal of Nanoscience and Nanotechnology, 2016, 16, 3364-3367.	0.9	Ο
250	Carrier Transport Mechanism in Single Crystalline Organic Semiconductor Thin Film Elucidated by Visualized Carrier Motion. Journal of Nanoscience and Nanotechnology, 2016, 16, 3388-3393.	0.9	0
251	A Special Section on Recent Progress in Nano-Molecular Electronics. Journal of Nanoscience and Nanotechnology, 2016, 16, 3157-3158.	0.9	Ο
252	A Novel Microscopic Analyzing System for Characterizing Organic Lightâ€Emitting Diodes Using EFISHG and LBIC Measurements. Electronics and Communications in Japan, 2017, 100, 76-83.	0.5	0

#	Article	IF	CITATIONS
253	Probing Internal Electric Field in Organic Photoconductors by Using Electric-Field-Induced Optical Second-Harmonic Generation. IEICE Transactions on Electronics, 2019, E102.C, 113-118.	0.6	0
254	Visualization of Carrier Transport in Organic-Inorganic Perovskite Field-Effect Transistor by Electric-Field-Induced Optical Second-Harmonic Generation (EFISHG). , 2019, , .		0
255	Visualization of Carrier Transport in Luminescent Polymer Thin Film by Using Transient Photoluminescence Decay Imaging. Physica Status Solidi (A) Applications and Materials Science, 2020, 217, 1901031.	1.8	0
256	Study of Electron Injection of Pentacene Field Effect Transistor with Au Electrodes by C-V and SHG Measurements. Transactions on Electrical and Electronic Materials, 2008, 9, 151-155.	1.9	0
257	Morphological Evidence of Chirality in Poly (diacetylene) Film Prepared Using Circularly Polarized Light. International Journal of the Society of Materials Engineering for Resources, 2010, 17, 193-196.	0.1	0
258	Probing of Maxwell-Wagner Type Interfacial Charging Process in Double-Layer Devices by Time-Resolved Second Harmonic Generation. IEICE Transactions on Electronics, 2011, E94-C, 141-145.	0.6	0
259	Analyzing Two Electroluminescence Modes of ITO/α-NPD/Alq <sub>3</sub> /Al Devices by Using A.C. Square Voltages. IEEJ Transactions on Electronics, Information and Systems, 2012, 132, 1408-1412.	0.2	0
260	Investigation of Interfacial Charging Process of Pentacene/C <sub>60</sub> /BCP Triple-Layer Organic Solar Cells. IEICE Transactions on Electronics, 2013, E96.C, 358-361.	0.6	0
261	Mobility Control of TIPS-Pentacene Thin Films Prepared by Blade-Coating Method. IEICE Transactions on Electronics, 2017, E100.C, 130-132.	0.6	0
262	A Novel Microscopic Analyzing System for Characterizing Organic Light-emitting Diodes using EFISHG and LBIC Measurements. IEEJ Transactions on Fundamentals and Materials, 2017, 137, 128-134.	0.2	0